Progress toward a new measurement of the parity violating asymmetry in $\vec{n} + p \rightarrow d + \gamma$

W.M. Snow [a], W.S. Wilburn [b], J.D. Bowman [b],
M.B. Leuschner [c], S.I. Penttilä [b], V.R. Pomeroy [c], D.R. Rich [a],
E.I. Sharapov [d], and V. Yuan [b]

[a] *Department of Physics, Indiana University, Bloomington, Indiana 47405*

[b] *Los Alamos National Laboratory, Los Alamos, New Mexico 87545*

[c] *Department of Physics, University of New Hampshire, Durham, New Hampshire 38245*

[d] *Joint Institute for Nuclear Research, 141980 Dubna, Russia*

Abstract

We outline the motivation and conceptual design for a new experiment aimed at a 10-fold improvement in the accuracy of the parity-violating asymmetry A_γ in the angular distribution of 2.2 MeV gamma rays from the $\vec{n} + p \rightarrow d + \gamma$ reaction. This observable is primarily sensitive to the weak pion-nucleon coupling H_π^1. A proof-of-principle experiment using unpolarized low-energy neutron capture on polyethylene and an array of 12 CsI detectors operated in current mode has been performed. Results of this test experiment including the current mode signal, electronic noise and detector sensitivity to magnetic fields are reported.

1 Motivation

The flavor-conserving quark-quark weak interaction remains the most poorly tested aspect of the electroweak theory. One can judge the slow rate of progress in our understanding of this sector by noting the similar state of affairs described in two reviews of the subject conducted a decade apart [1,2]. The reasons for the slow advance are both theoretical and experimental. The experimental problems stem from the small size of weak amplitudes relative to strong amplitudes (typically $\approx 10^{-7}$ at low energies). The theoretical difficulties are encountered in trying to relate the underlying electroweak currents to low-energy observables in the strongly interacting regime of QCD. The current approach is to split the problem into two parts. The first step is to map QCD

to an effective theory expressed in terms of the important degrees of free-dom of low energy QCD, mesons and nucleons. In this process, the effects of quark-quark weak currents appear as parity-violating meson-nucleon-nucleon couplings [3]. The second step is to use this effective theory to calculate elec-troweak effects in the NN interaction and to determine the weak couplings from experiments.

A naive analysis of the structure of the quark-quark weak current implies that the isovector part of the weak current should be strongly dominated by the neutral current contribution. In terms of the meson-exchange picture of the weak NN interaction, this means that the weak pion exchange is partic-ularly interesting, since it should be dominated by neutral currents. It is also the longest range component of the weak NN interaction, and therefore pre-sumably the most reliably calculable in the NN system. Finally, it is worth pointing out that the exchange of neutral currents between quarks has never been isolated experimentally. For all of these reasons, the coupling constant for the weak π exchange, H_π^1, is of special interest [1] .

The size of H_π^1 is not known. The most reliable information on the strength of H_π^1 is believed to come from measurements of the circular polarization of 1081 keV gamma rays from ^{18}F [4]. The current results have been inter-preted as an upper limit of the weak pion-nucleon-nucleon coupling, $H_\pi^1 \leq 3.4 \times 10^{-7}$. This value is 3σ smaller than the expected value from the theory, $H_\pi^1 = 10.8 \times 10^{-7}$ (DDH "best value" [3]). This result has led to speculation that quark-quark neutral currents might be suppressed in $\Delta I = 1$ processes. New information on H_π^1 comes from the recent observation of nuclear parity violation in an atomic parity-violation experiment in ^{133}Cs [5]. This experi-ment detected for the first time the parity-violating nuclear anapole moment. Theoretical estimate for the value of H_π^1 inferred from this experiment, is $H_\pi^1 = 22.6 \pm 5.0(\text{exp.}) \pm 8.3(\text{theor.}) \times 10^{-7}$ [6], which is significantly larger than the upper limit set by the ^{18}F experiments. This disagreement is almost certainly due to problems in the nuclear structure calculations necessary to extract H_π^1 from these measurements, and there is speculation that H_π^1 may be modified in the nuclear medium [7]. At the same time, the DDH prediction for H_π^1 has sharpened to 0–6 $\times 10^{-7}$ [8] due to improved knowledge of the QCD coupling constant and the treatment of quark masses.

An accurate measurement in the nucleon-nucleon system sensitive to H_π^1 is needed to resolve these inconsistencies. The NN system is simple enough that the measured asymmetry can be related to the weak meson-nucleon-nucleon coupling with negligible uncertainty to nuclear structure. Parity vi-olation in the neutron-proton system is primarily sensitive to weak π- and

---

[1] We have used the notation of Adelberger and Haxton [1], where $H_\pi^1 = F_\pi = g_\pi f_\pi/\sqrt{32}$, $H_\rho^1 = F_1 = -g_\rho h_\rho^1/2$, $H_\omega^1 = G_1 = -g_\omega h_\omega^1/2$ and $H_\rho'^1 = H_1 = -g_\rho h_\rho'^1/4$.

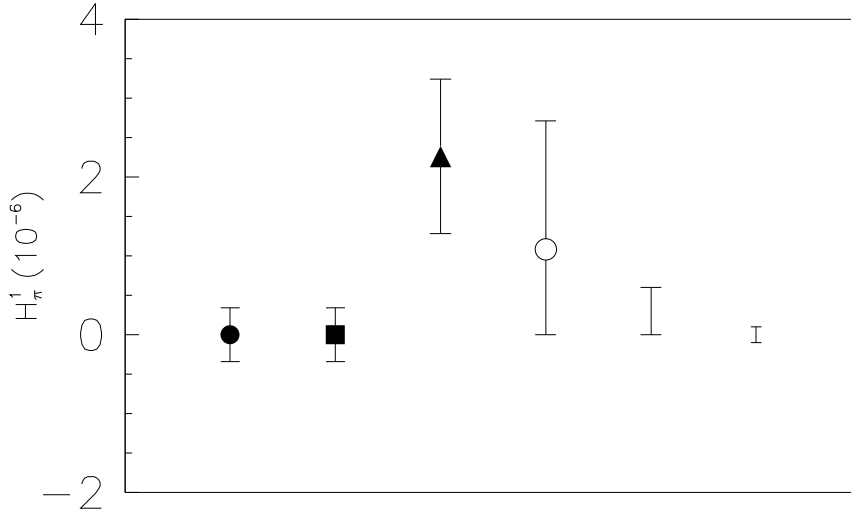Fig. 1. Values of H_π^1 from (left to right) the earlier $\vec{n} + p \rightarrow d + \gamma$ experiment, ^{18}F experiments, ^{133}Cs experiment, DDH theoretical estimate, and Desplanques theoretical estimate. The last value represents the expected uncertainty from the proposed experiment. References and explanation are found in the text.

ρ-exchange, which are the longest-range contributions. An analysis of the available low-energy channels in the neutron-proton system indicates [1] that parity-nonconserving (PNC) effects in the reaction $\vec{n} + p \rightarrow d + \gamma$ are almost entirely due to the weak pion exchange.

The relationship between the PNC asymmetry A_γ and H_π^1, where A_γ is the correlation between the direction of emission of the gamma ray and the neutron polarization, is calculated to be [1]

$$A_\gamma = -0.045 \left(H_\pi^1 - 0.02 H_\rho^1 + 0.02 H_\omega^1 + 0.04 H_\rho^{'1} \right). \tag{1}$$

This result is consistent on the coefficient of H_π^1 with an earlier calculation by Desplanques and Missimer [9]. The final result from the last experiment [10] was $A_\gamma = -1.5 \pm 4.8 \times 10^{-8}$ [11]. This value is neither sensitive enough to address the inconsistencies in the size of H_π^1, or to reach the range of values for H_π^1 predicted by theories [3,12,13].

In this paper, we discuss a new experiment to measure A_γ to a precision of $\pm 5 \times 10^{-9}$ which will determine H_π^1 to $\pm 1 \times 10^{-7}$ (see figure 1). Such a result will clearly distinguish between the ^{18}F and ^{133}Cs values for H_π^1 as well as between different predictions given by theories of the weak interaction of hadrons in the non-perturbative QCD regime. There is also a strong possibility that a non-zero result will be seen and that the value of H_π^1 will finally be known.

2   Requirements for an Accurate Measurement of A_γ in the Reaction $\vec{n} + p \rightarrow d + \gamma$

To determine H_π^1 with an uncertainty of 1.0×10^{-7}, 10% of the DDH best value, we need a statistical uncertainty of 0.5×10^{-8} on A_γ which means that we have to detect about 4×10^{16} gammas from the $\vec{n} + p \rightarrow d + \gamma$ reaction. On the other hand, we have to keep the systematic errors below the statistical error. Among the essential aspects of the proposed experiment which led us to the choice of issues to be addressed in the proof-of-principle experiment, are the following:

(i) The number of events required to achieve sufficient statistical accuracy in a reasonable time immediately leads to the conclusion that the 2.2 MeV gamma rays must be counted in current mode.

(ii) Neutron fluxes available at present neutron sources are not high enough to achieve the required statistical accuracy in a small amount of time. Therefore, it is important to demonstrate that the electronic noise introduced by the current-mode measurement technique is negligible compared to the shot noise due to the discrete nature of the charge deposited by each gamma ray and number of photoelectrons produced by the neutron capture event.

(iii) The tiny parity violating signal will be isolated by flipping the neutron spin, since the real asymmetry will change sign under spin reversal, while spin-independent false asymmetries will not. The neutron spin can be flipped by either static or RF magnetic fields. It is essential to measure the sensitivity of the detector efficiency to magnetic fields and show that the systematic effect introduced by the magnetic fields to the asymmetry is much smaller than the statistical error.

There are a host of other issues to be addressed, including systematic effects, production and delivery of the polarized neutrons to the protons, the details of the neutron spin flipping, etc. However, the three issues mentioned above would render the experiment impossible if unresolved. Therefore we constructed an experiment to address these questions.

3   Experiment

A proof-of-principle test run was performed at the pulsed spallation source of the Los Alamos Neutron Science Center (LANSCE) where neutrons are produced by impinging 800 MeV proton pulses at the repetition rate of 20 Hz from the Proton Storage Ring to the tungsten spallation target surrounded by a water moderator. The neutron yield from the moderator surface has a

Maxwell-Boltzmann low-energy component and a high-energy tail which falls off as $1/E$. The peak of the neutron flux, 4×10^{13} eV^{-1}·s^{-1}·sr^{-1}), is at about 4 meV [14]. The intensity of the neutron flux at the moderator surface at epithermal energies is approximately given by

$$\frac{d^2 N}{dt\, dE} \approx \frac{N_0 f \Omega}{E}. \tag{2}$$

Here $N_0 = 2 \times 10^{12}$ s^{-1}·sr^{-1}, f is the fraction of the 13 cm by 13 cm moderator viewed by the collimator system, and Ω is the solid angle. The experiment was mounted 6 m from the source and using the time-of-flight method the incident neutrons at an energy range below 1 eV were detected. This energy range was selected so that the 2.2 MeV gamma rates on the detector would correspond to the rates from the cold neutron moderator at the parity-violating experiment. The neutrons were additionally thermalized in a polyethylene sample to take advantage of the larger capture cross section on a proton for the thermal neutrons.

Figure 2 shows the number of capture gammas from the polyethylene target as a function of neutron a time-of-flight (t.o.f. for 1 eV neutrons is about 440 μs at 6 m) after the beam has passed through a 0.3 mm thick indium foil and a 1.5 mm thick aluminum plate. The signals were taken from the photocathodes of the photomultiplier tubes and then multiplied with preamplifiers. The first goal of the test experiment was to verify that in the current-mode operation the electronic noise of the detector system can be reduced below the shot noise; the statistical fluctuations of the current due to the finiteness of the deposited energy of the gammas or the number of photoelectrons produced per event. The second goal of the test experiment was to measure the sensitivity of the detector efficiencies to magnetic fields. For these tests an array of 12 CsI detectors were used.

In the test experiment, a 15 cm diameter by 5 cm thick target of polyethylene, supported by a 2 cm thick cylindrical polyethylene shell, was placed in a 10 cm diameter neutron beam. The 12 CsI(pure) crystals were arranged around the target in an annulus having an inner diameter of 20 cm, an outer diameter of 40 cm, and a length of 13 cm [15]. The detector array was centered approximately 6 m from the spallation neutron source and subtended a solid angle of 3.0 sr relative to the target. This arrangement is shown schematically in figure 3. The detector system was mounted inside a 10 cm thick lead housing with holes for the beam entry and exit. The scintillation light from the CsI crystals was viewed directly by individual phototubes (Hamamatsu R5004). Signals were taken from the photocathodes. All other phototube elements, including dynodes, were connected to a battery and biased to +90 V with respect to the cathodes.
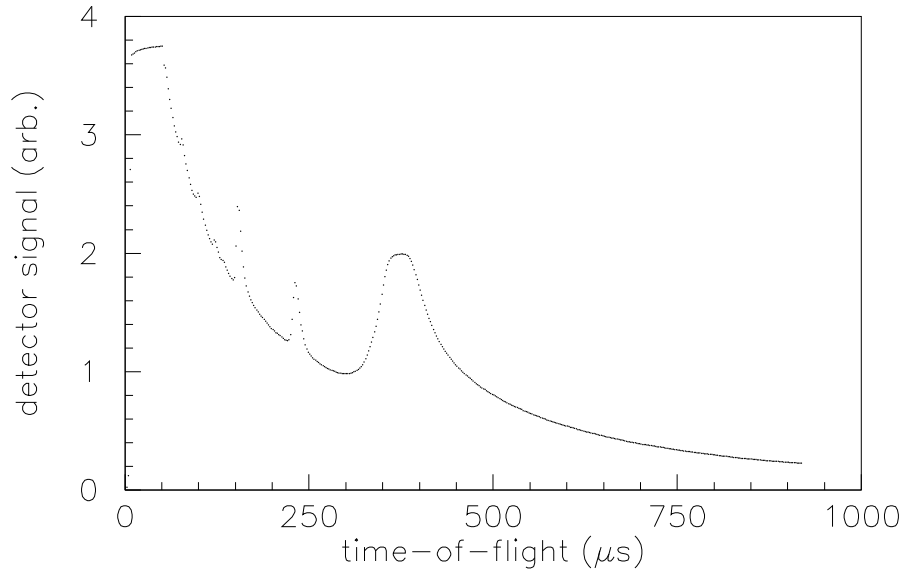
Fig. 2. Gammas from neutron capture on polyethylene as a function of neutron time-of-flight. The neutron beam passes through 0.3 mm In and 1.5 mm Al before impinging on the target.
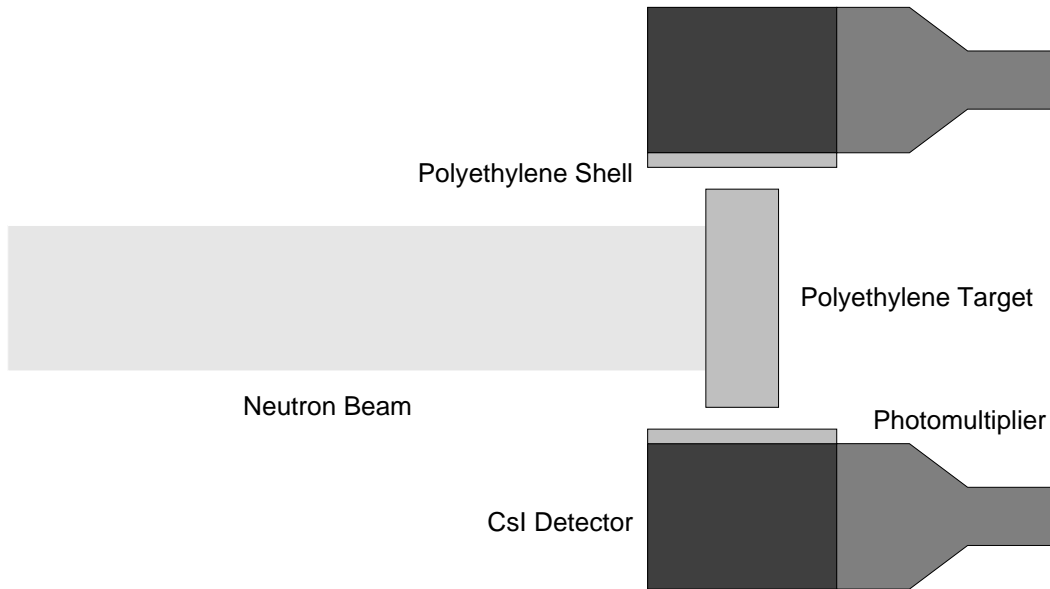

Fig. 3. Experimental arrangement for the test experiment, showing the neutron beam, polyethylene target, and CsI detectors.

Two different electronic configurations were tested. In the first, only two individual photocathodes were connected to low-noise preamplifiers attached directly to the phototube sockets. The amplified signals then went to a NIM module which formed sum and difference signals. This arrangement was used to measure the electronic noise and is similar to design for the proposed mea-

surement, where each photocathode will have an individual preamplifier. In the second configuration, the detector photocathodes were connected together in two groups of six; top and bottom. The two signals from each group were amplified and then they went to the summing and differential amplifiers, as described above. This circuit was used to study fluctuations in the capture gamma flux, due to effects such as beam intensity and position modulations. With this circuit, we could measure the spectral density of the beam noise.

The detector electronics used for the noise measurements are shown in figure 4. The circuit consists of two low-noise current-to-voltage (IV) amplifiers, followed by stages which take the sum and difference of the two voltages. The IV amplifiers were designed using AD745A op-amps. These op-amps have a typical voltage noise density of 2.9 nV/$\sqrt{\text{Hz}}$ and typical current noise density of 6.9 fA/$\sqrt{\text{Hz}}$ at 1 kHz. The 10 MΩ feedback resistor gives a DC gain of 10 V/μA. A 10 pF feedback capacitor combined with an external low-pass filter limit the 3 dB bandwidth to 3.0 kHz. This corresponds to a time constant of approximately 50 μs. Precision resistors (0.1%) with low temperature coefficients (20 ppm/°C) are used in the IV, summing, and differential amplifier stages. The summing circuit was designed to have an overall gain of 10 V/μA, and the differential circuit a gain of 1.0 V/nA. The spectral density measurement used the same circuit with the preamplifier gain reduced by a factor of 50 and the bandwidth increased to 160 kHz.

3.1 Current Mode Signal

Several measurements were performed to ensure that the observed detector current for the full array, 0.56 μA for 1 eV neutrons, was consistent with calculations based on neutron capture gamma rays from hydrogen in the polyethylene target. This number is the product of the neutron flux, probability for the neutron to capture on a proton, probability that the capture produces a gamma ray which absorbs in the detector, and the charge per gamma ray which appears at the photocathode. The instantaneous flux of 1 eV neutrons on the target could not easily be measured directly. Instead, a flux of 5×10^{10} s^{-1} was inferred from a measurement of the count rate in a ^{6}Li-loaded glass scintillator 1 cm thick and 1 cm in diameter located 56 m from the spallation source. The observed count rate of 10.8 kHz was low enough to use the normal pulse-counting method.

A Monte Carlo calculation was performed to estimate the fraction (approximately 60%) of incident neutrons which capture on protons in the polyethylene target after moderation. Most of the remaining neutrons backscatter from the target. The mean free path of 5 mm for thermal neutrons in polyethylene was used in the calculations and was verified by relative transmission measure-
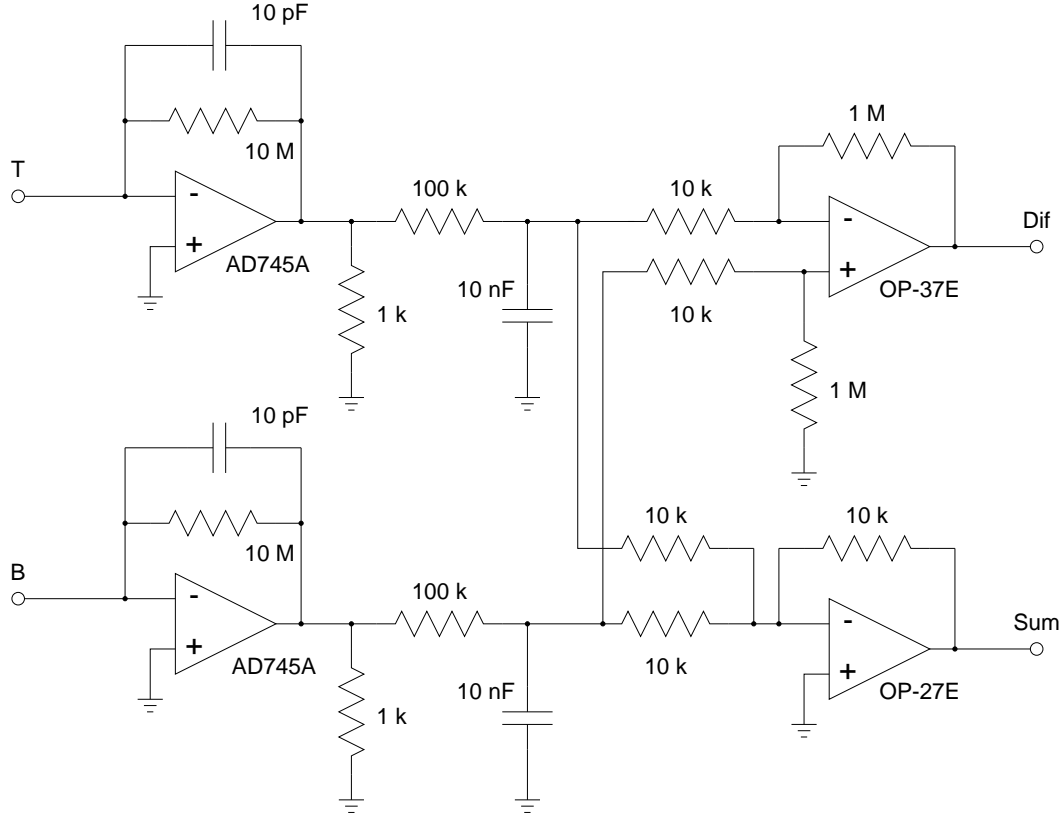
Fig. 4. Diagram of the detector front-end electronics for the test experiment.

ments. The prediction for the amount of backscattered neutrons was tested by moving the location of the target relative to the detector array and observing that the target position which gave the largest detector signal was located about 6 cm downstream from the center of the detector annulus. The large size of the signal at this position, about 2.5 times larger than the signal for the target centered on the array, was attributed to backscattered neutrons which capture on the protons in the cylindrical polyethylene support structure for the target (gamma rays from the support are closer to the detectors and have a larger solid angle).

Since the solid angle was known, the only remaining quantity needed to calculate for the detector current was the number of photoelectrons produced in the photocathodes of the CsI detectors by the 2.23 MeV gamma ray. This number was determined by two independent methods. First, the polyethylene target was replaced by a 0.3 mm thick In foil. At 1.46 eV indium possesses a strong neutron resonance which captures all the neutrons from the beam. The resonance state decays primarily *via* gamma emission. Using the measured detector current at the resonance, we inferred a value of 70 photoelectrons per MeV of deposited gamma ray energy. This number was consistent within errors with the value of 65 photoelectrons per MeV inferred from the energy resolution measurement of the CsI detectors with a ^{60}Co gamma source. The

number of photoelectrons per MeV was calculated under the assumption that the energy resolution is dominated by the statistical fluctuations of the number of photoelectrons.

Based on this combination of measurements and simulations, the predicted detector current for the full array of 12 detectors is about 0.5 ± 0.1 μA for 1 eV neutron rate. The agreement with the measured value of 0.56 μA has two consequences: 1) the current-mode signal is indeed dominated by gamma rays from neutron capture on protons, 2) the value for the number of photoelectrons per MeV in the detector is determined. This value is needed to calculate the expected amount of noise in the detector array due to current shot noise from neutron counting statistics.

3.2   Electronic Noise

Using a digital oscilloscope (LeCroy model TDS 744A) the electronic noise of the detector was determined for the sum and difference outputs. The noise of the sum output was 760 μV$_{\mathrm{rms}}$. Referred to the input, this corresponds to 1.4 pA/$\sqrt{\mathrm{Hz}}$. The difference output had 110 μV$_{\mathrm{rms}}$ noise, corresponding to 0.2 pA/$\sqrt{\mathrm{Hz}}$ at the input. It is useful to compare the difference noise to the rms shot noise created by the quantized nature of the expected detector signal

$$I_{sn}/\sqrt{f} = \sqrt{2qI}, \tag{3}$$

where q is the charge generated in the photocathode per gamma and I is the photocathode current. Using the expected values $q \approx 150e$ and $I \approx 100$ nA, we obtain $I_{sn}/\sqrt{f} \approx 2$ pA/$\sqrt{\mathrm{Hz}}$, a factor of 10 greater than our electronic noise. Calculations with a SPICE model of the preamplifier indicate that an electronic noise of just 13 fA/$\sqrt{\mathrm{Hz}}$ should be obtainable. We attribute the excess noise observed in our test to be from electromagnetic pickup. This contribution will be reduced with improved electrostatic shielding.

3.3   Spectral Density

Periodic variations in experimental parameters can produce false asymmetries. These effects include fluctuations in detector gain, beam intensity and beam position, which are expected to dominate over other fluctuations. The proposed experiment has been designed so that these fluctuations do not contribute to a false asymmetry in first order. Since the parity-violating asymmetry is formed by taking the difference between up and down detector currents, the two currents are measured simultaneously, making the apparatus

quite insensitive to incident flux variations. Second, the azimuthal symmetry of the apparatus suppresses the contribution from the beam motion. While such effects do not lead directly to false asymmetries, it is possible for them to contribute in higher order. For example, the beam motion combined with detector-efficiency differences can give a non-zero effect. For this reason, it is important to know the size of the beam fluctuations.

We measured the influence of these fluctuations on the detector signal and set an upper limit for their contribution. We sampled the difference signal from the detectors every 50 ms (every beam pulse) by integrating the voltage for 1μs for a 20 minute period while the spallation source operated in a steady-state mode. The autocorrelation function of the difference signal, $f(\tau) = \langle i(t)i(t-\tau)\rangle$ was then calculated. The Fourier transform of this quantity, $F(\omega) = \int_{-\infty}^{+\infty} f(\tau)e^{i\omega\tau}d\tau$, is the spectral density of the intensity fluctuations of the neutron source as filtered through the difference signal. There were no periodic sources of noise observed in the 0–10 Hz range (fig. 5). The upper limit of this range is set by the sampling rate, which is in turn limited by the pulse spacing. Because the circuit bandwidth (160 kHz) was larger than this upper observable frequency, the noise above 10 Hz is aliased into the 0–10 Hz range. Correcting for this effect, we estimate an upper limit of 5 fA/$\sqrt{\text{Hz}}$ on beam-induced fluctuations on the difference signal.
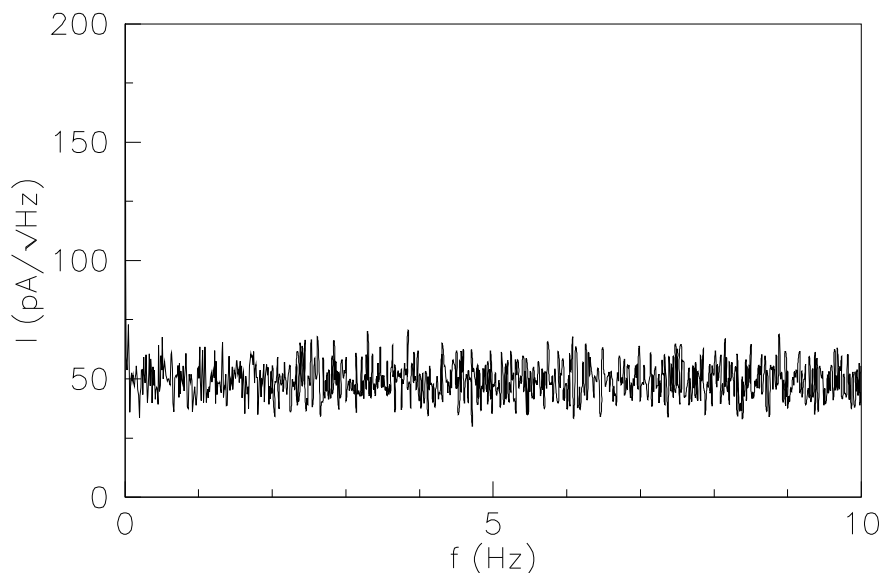

Fig. 5. Spectral density of the detector difference signal, due to fluctuations in the neutron beam parameters.

The primary techniques for reducing the false asymmetries generated by the experimental fluctuations is the fast reversal of the neutron spin. Depending on the reversal techniques it will introduce changing magnetic fields which can effect the efficiency of the detector. Therefore it was important to measure the sensitivity of the detector to magnetic fields. The measurement was performed by applying a 10 gauss magnetic field to the detectors using a pair of 76 cm diameter coils. The field direction was reversed every 10 s. The field was oriented parallel to the photocathode surfaces of the photomultiplier tubes in an attempt to maximize the size of the effect. The observed change in the detector efficiency was 2×10^{-5} per gauss. This is about five orders of magnitude smaller than one would expect for a typical photomultiplier tube operated in the normal fashion with high voltage on the dynodes and the signal measured from the anode. The observed field sensitivity can be reduced further through the use of special photocathode materials.

Changes in static magnetic fields at the detectors upon a spin flip must therefore be held below the 10 μgauss level. Spin flipping by RF magnetic fields would be preferable, since one expects the detectors and associated electronics to be even less sensitive to such fields and one can shield RF magnetic fields effectively.

The conclusions of the test measurements are that the noise introduced by the current-mode detection is less than the shot noise and the magnetic field sensitivity of the detector is very low when the signals are taken from the photocathodes.

In the remainder of the paper, we discuss a conceptual design of the experiment based on the results of the test experiment, an estimate for the statistical accuracy, and diagnostics for some classes of systematic effects.

4   Conceptual Design of $\vec{n} + p \rightarrow d + \gamma$ Experiment

We briefly describe in this section a conceptual design of the $\vec{n} + p \rightarrow d + \gamma$ experiment. Figure 6 shows the elements of the design. Next we discuss those aspects which are particularly important for the experiment.

The experiment requires a high flux of cold neutrons with energies below 15 meV, as will be explained later. While such neutrons are available from cold moderators at both reactors and spallation neutron sources, the pulsed nature of the neutron flux from a pulsed spallation source provides a very
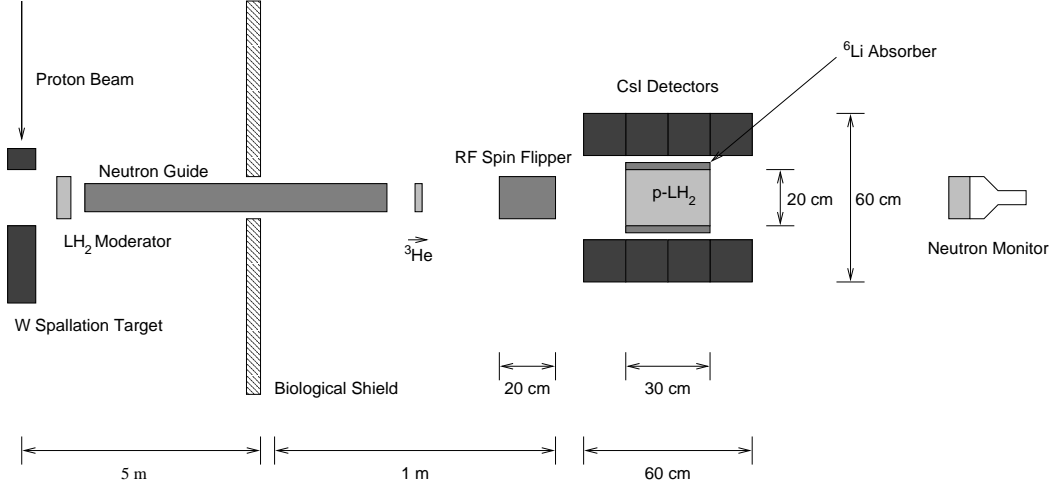
Fig. 6. The conceptual design for the $\vec{n} + p \to d + \gamma$ experiment, showing the most important elements (not to scale). Approximate sizes and distances are indicated for some features.

powerful diagnostic tool for a number of systematic effects for this experiment. At LANSCE the cold neutron source consists of a liquid hydrogen moderator coupled to the 20 Hz pulsed neutron source. The neutron spectrum consists of a Maxwellian component with a maximum at 4 meV and width set by the effective temperature of the moderator (approximately 50 K) and a higher energy component of "under-moderated" neutrons with an approximately $1/E$ spectrum (figure 7). Approximately 90% of the neutrons possess energies below 15 meV [16].

The intensity of neutrons from an isotropic source falls off as $1/R^2$. At cold neutron energies, however, it is possible to use neutron guides to transport neutrons. The neutron guide possess a reflectivity which is close to unity for neutrons incident at glancing angles below a critical angle θ_c, and the reflectivity falls sharply above this angle. The function of the neutron guide is to conserve the high neutron flux available near the moderator. Since the θ_c depends on neutron energy, the guide increases the flux at lower neutron energies compared to the neutron transmission without the guide.

The experiment requires polarized neutrons. We plan to use a polarized ^{3}He neutron-spin filter [17,18]. Polarized ^{3}He gas acts as a transmission polarizer. The total cross section for the ^{3}He nucleus is very large for the $J = 0$ capture channel, which decays mostly by breakup to a triton and proton, and about four orders of magnitude smaller for the $J = 1$ channel. The neutron polarization (P) and transmission (T) properties are therefore strongly dependent on ^{3}He polarization: an example is shown in figure 8.

The parity-violating signal will be isolated by periodically reversing the neutron spin. The spin flipper must be capable of rapidly and reproducibly reversing the beam polarization in a broad range of cold neutron energies with
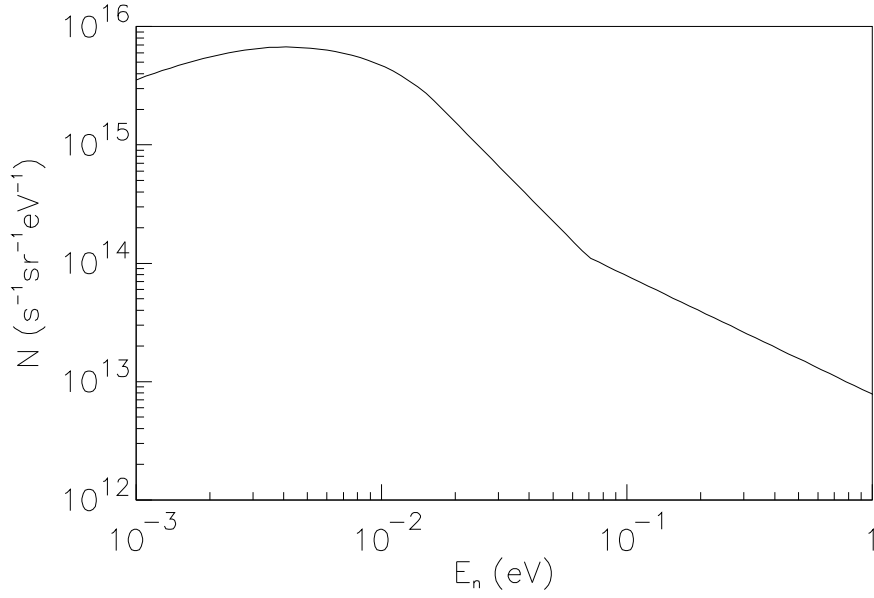
12

Fig. 7. Neutron flux from the LANSCE coupled cold moderator. This is the total neutron flux from the 13 cm by 13 cm moderator surface with the average proton current of 200 μA.
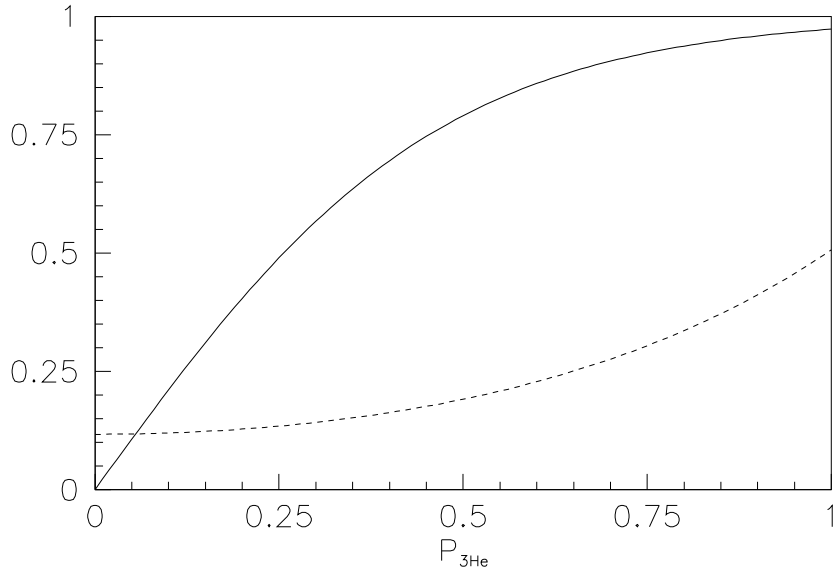

Fig. 8. Polarization (solid) and transmission (dash) of 4 meV neutrons after passage through a 6 atm·cm ^{3}He cell, as a function of ^{3}He polarization.

essentially unit efficiency over the entire beam profile with no effect on the gamma detectors. The fast (20 Hz) spin reversal is possible with a spin flipper which uses RF magnetic fields [19]. The reversal of the neutron polarization then consists of turning the RF magnetic field on and off, which can be done

quickly enough to flip the neutron polarization on every beam burst at 20 Hz. The gamma detectors can be efficiently shielded from the RF magnetic field with a thin metal enclosure. Neutron spin flippers based on the reversal of an otherwise static magnetic field suffer primarily from the greater difficulties of shielding static magnetic fields and the relatively higher sensitivity of the gamma detector efficiency to static fields.

In order for the experiment to be clearly interpretable as a measurement of parity violation in the neutron-proton system, a target of pure hydrogen is required. Clearly, it is essential that the polarized neutrons retain their polarization until they capture. It is therefore important to consider the spin dependence of the scattering.

The ground state, the para state, of the hydrogen molecule has $J = L = S = 0$, and the first excited state, the lowest ortho state, is at 15 meV above the para state. A large fraction of the cold neutrons possess energies lower than 15 meV. Since these neutrons cannot excite the para-hydrogen molecule, only elastic scattering and capture are allowed, and spin-flip scattering is forbidden. The neutron polarization therefore survives the large number of scattering events which occur before the capture. Higher energy neutrons will undergo spin-flip scattering and will therefore depolarize. This is the reason for the requirement of neutrons with energies below 15 meV.

We must prepare a liquid hydrogen target in the para state. For liquid hydrogen held at 20 K and atmospheric pressure the equilibrium concentration of para-hydrogen is 99.8%, low enough to ensure a negligible population of ortho-hydrogen.

Finally, we must detect the 2.2 MeV gamma rays from neutron capture. Given the small size of the expected asymmetry and gamma-detector dead times, the required counting rates for a practical experiment are too great for pulse counting. Current-mode gamma detection is therefore required. In addition, the gamma detector must cover a large solid angle with a high, time-independent efficiency which is unaffected by neutron spin reversal and radiation damage.

Segmentation of the detector is required to resolve the angular dependence of the expected parity-violating signal and discriminate false effects. For example, there is a predicted parity-conserving gamma asymmetry of $A_\gamma^{PC} = 7 \times 10^{-9}$ [20] in the np capture. This process gives an asymmetry about the same magnitude as our sensitivity goal for the parity violating signal, but with an angular distribution orthogonal to the parity violating signal. Some degree of segmentation is therefore necessary to separate the parity-violating and parity-conserving asymmetries.

The alkali iodine crystals are well suited for the gamma ray detection because of their high density, 4.5 g/cm^3. Three interaction lengths (3×5.5 cm) thick
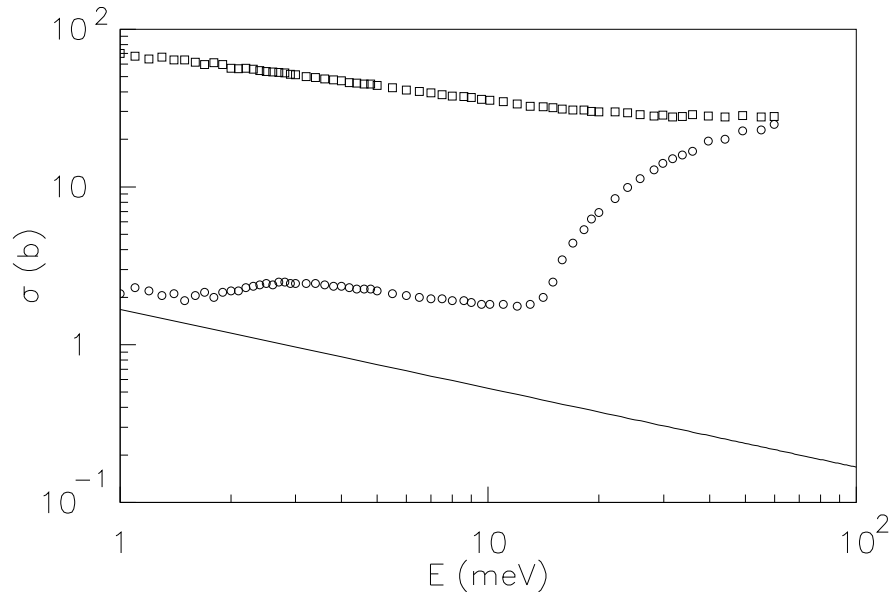
Fig. 9. Measured scattering cross sections for neutrons on para-hydrogen (solid) and neutrons on normal hydrogen (dash). The solid line is the cross section for the np capture.

crystal will stop 95 % of the 2.2 MeV gamma rays. Our plan is to use cubes of CsI(Tl) crystals approximately 15 cm on a side coupled to photomultiplier tubes operated in current mode. The signal is taken directly from the photo-cathode to decrease the sensitivity of detector gain to magnetic fields, as in the test experiment. Similar detectors have been observed to have acceptably low gain drifts ($< 1\%$ per week [21]). Based on previous studies, these detectors should be capable of withstanding the integrated gamma dose in the experiment without serious effects on the detector efficiency [22]. They were used successfully in our test runs to perform current-mode counting at the expected instantaneous rates of 10^{11} gammas per second.

The gamma detectors must be shielded from neutrons scattered from the hydrogen target. ^{6}Li is the ideal material for this purpose due to its large neutron absorption cross section, most of which proceeds by a breakup channel to a triton and alpha in their ground states, thus producing no gamma rays.

In addition to its primary purpose of measuring the beam intensity, the beam monitor can be used to detect changes in the concentrations of ortho-hydrogen and para-hydrogen in the target. This is possible due to the very large difference in neutron cross sections for the two species at low neutron energies (see Figure 9) [23,24]. At 4 meV neutron energy, for example, the ortho-hydrogen cross section is 20 times larger than the para-hydrogen cross section. Even small changes in the 0.2% equilibrium ortho-hydrogen concentration in the target will therefore lead to large changes in the transmitted neutron flux.

15

Next we estimate briefly the statistical accuracy of the experiment achievable with the LANSCE neutron sources described above. The estimate has been done under the following assumptions:

(i) The time-averaged brightness from a coupled liquid hydrogen moderator at the (upgraded) LANSCE proton beam current of 200 μA peaks at 4 meV at a value 6×10^{15} neutrons/(eV·s·sr) (see figure 7).

(ii) A 5 m, 10 cm×10 cm multi-layer neutron guide is mounted 1 m from the moderator. The transmission of the guide is assumed to be 100% for neutrons with angles of incidence with the guide surface smaller than $2\theta_c$.

(iii) A polarized ^{3}He neutron polarizer with 65% ^{3}He polarization and 4.5 atm·cm of gas.

(iv) A 30 cm long, 30 cm diameter cylindrical liquid para-hydrogen target, which converts approximately 60% of the incident neutrons to gamma rays according to MCNP calculations.

(v) The CsI(Tl) gamma detectors are used only to determine which hemisphere the gamma ray enters.

(vi) The gamma detectors cover 4π solid angle.

(vii) The uncertainty in the gamma flux striking detectors, operated in current mode, is dominated by gamma ray counting statistics.

Under these assumptions, a Monte Carlo simulation gives a statistical error in the gamma asymmetry in one year of counting of 5.8×10^{-9}. This statistical accuracy suffices to reach the goal of the experiment.

5   About Systematic Uncertainties

The most challenging aspect of the experiment is to design an apparatus which is a) insensitive to spurious systematic effects, b) incorporates a large number of independent methods to isolate a true parity-violating signal, and c) is flexible enough to allow the size of as many systematic effects as possible to be magnified artificially. The most dangerous class of systematic effects are those correlated with the neutron spin reversal, either through the direct physical effects due to the interaction of the neutron spin itself or through indirect effects on the gamma ray detection efficiency correlated with the neutron spin flipping process.

A detailed analysis of systematic effects lies outside the scope of this paper. However, we can point to aspects of the design of the experiment which are important for the study and isolation of systematic effects.

At a pulsed neutron source, the arrival time of the neutron at the experiment after the proton pulse strikes the spallation target depends on the neutron

16

energy: $t \propto 1/\sqrt{E}$. The relation between the neutron energy and the timing of the gamma ray signal is blurred somewhat by the distribution of moderation times of the neutrons first in the LH_2 moderator of the spallation source and then in the hydrogen target (which averages about 100 μs), but this effect is small in comparison to the flight times of the neutrons of interest (for instance, a 4 meV neutron needs 9 ms for a 8 m flight). Therefore, the time dependence of the gamma ray signal can be correlated with the incoming neutron energies.

The time-of-flight information is very useful for isolating and identifying systematic effects simply because different effects possess different dependences on neutron energy. For example, a systematic effect associated with the neutron beam motion due to the Stern-Gerlach effect in a gradient magnetic field in the spin transport system grows as the square of the time spent in the field gradient, and thus increases as a function of time-of-flight. On the other hand, a systematic effect from parity-conserving left-right scattering asymmetries coupled to detector asymmetries grows with the incident neutron energy and therefore decreases with time-of-flight. Each systematic effect has a characteristic time signature which can be used as a partial means of identification. Most of these time signatures are different from that expected from the true signal.

As noted in section 4, neutrons with energies above 15 meV tend to depolarize before they capture. This not only effectively turns off the parity violating signal, but also all systematic effects which require the neutrons to be polarized in the para-hydrogen target. For example, effects induced by left-right scattering asymmetries in para-hydrogen must vanish above 15 meV. On the other hand, systematic effects not associated with polarized neutrons on hydrogen, such as bremsstrahlung from the parity-violating beta decay of window materials of the LH_2 target cryostat, will still be present at neutron energies above 15 meV.

6   Conclusions and Summary

A sensitive measurement of the parity-violating gamma asymmetry in the reaction $\vec{n} + p \rightarrow d + \gamma$ can give definitive information on one of the most important and interesting components of the weak NN interaction. We have successfully tested a current-mode detector concept for the gamma rays and verified that its precision is limited only by gamma ray counting statistics. We have demonstrated that the efficiency of our current-mode gamma detector is insensitive to changes in magnetic field, the most important external parameter used to change the sign of the parity-violating signal in the experiment. The realization of all other aspects of the experimental design appears to pose no insuperable technical difficulties. We have discussed a realistic experimental

design which has the potential to be free of systematic effects at the required level and incorporates a number of powerful diagnostics to isolate systematic effects.

We conclude that an experiment to search for the parity-violating gamma asymmetry in the reaction $\vec{n} + p \rightarrow d + \gamma$ with a sensitivity which is likely to obtain a nonzero result is now feasible.

7 Acknowledgments

References

[1] E. Adelberger and W. Haxton, Ann. Rev. Nucl. Part. Sci. **35**, 501 (1985).

[2] W. Haeberli and B. Holstein, in *Symmetries and Fundamental Interactions in Nuclei*, edited by W. Haxton and E. Henley (World Scientific, Singapore, 1995), p. 17.

[3] B. Desplanques, J. Donoghue, and B. Holstein, Ann. Phys. **124**, 449 (1980).

[4] S. Page *et al.*, Phys. Rev. C **35**, 1119 (1987).

[5] C. Wood *et al.*, Science **275**, 1759 (1997).

[6] V. Flambaum and D. Murray, Phys. Rev. C **56**, 1641 (1997).

[7] B. Desplanques, Phys. Rep. **297**, 1 (1998).

[8] B. Desplanques, in *Parity-Non-Conserving Nucleon-Nucleon Interactions*, edited by N. Auerbach and J. Bowman (World Scientific, Singapore, 1996), p. 98.

[9] B. Desplanques and J. Missimer, Nucl. Phys. **A300**, 286 (1978).

[10] J. Caviagnac, B. Vignon, and R. Wilson, Phys. Lett. **B67**, 148 (1977).

[11] J. Alberi *et al.*, Can. J. Phys. **66**, 542 (1988).

[12] E. Henley, W.-Y. Hwang, and L. Kisslinger, Phys. Lett. B **367**, 21 (1996).

[13] D. Kaplan and M. Savage, Nucl. Phys. **A556**, 653 (1993).

[14] P. Lisowski, C. Bowman, G. Russell, and S. Wender, Nucl. Sci. Eng. **106**, 208 (1990).

[15] C. Frankle *et al.*, in *Time Reversal Invariance and Parity Violation in Neutron Reactions*, edited by C. Gould, J. Bowman, and Y. Popov (World Scientific, Singapore, 1994), p. 204.

[16] P. Ferguson, private communication.

[17] K. Coulter *et al.*, Nucl. Instrum. Methods A **288**, 463 (1990).

[18] F. Tasset *et al.*, Physica B **180**, 896 (1992).

[19] S. Grigoriev, A. Okorokov, and V. Runov, Nucl. Instrum. Methods A **384**, 451 (1997).

[20] A. Csótó, B. Gibson, and G. Payne, Phys. Rev. C **56**, 631 (1997).

[21] E. Frlez *et al.*, Bull. Am. Phys. Soc. **42**, 994 (1997).

[22] Z. Wei and R. Zhu, Nucl. Instrum. Methods A **326**, 508 (1993).

[23] W. Seiffert, Technical Report No. EUR 4455d, Euratom (unpublished).

[24] W. Seiffert, B. Weckermann, and R. Misenta, Z. Naturforsch **25a**, 967 (1970).